UvA-DARE (Digital Academic Repository)

Plectin's actin-binding domain: a versatile element

Litjens, S.H.M.

Publication date
2006

Link to publication

Citation for published version (APA):
Litjens, S. H. M. (2006). *Plectin's actin-binding domain: a versatile element*. [Thesis, externally prepared, Universiteit van Amsterdam].

Modeling and Experimental Validation of the Binary Complex of the Plectin Actin-binding Domain and the First Pair of Fibronectin Type III (FNIII) Domains of the β4 Integrin*

Sandy H. M. Litjens‡, Kevin Wilhelmsen‡, José M. de Pereda§¶, Anastassis Perrakis‖, and Arnoud Sonnenberg‡**

From the Divisions of ‡Cell Biology, and ‖Molecular Carcinogenesis, The Netherlands Cancer Institute, Plesmanlaan 121, 1066 CX Amsterdam, The Netherlands and the §Centro de Investigacion del Cancer, University of Salamanca-CSIC, E-37007 Salamanca, Spain

The binding of plectin to the β4 subunit of the α6β4 integrin is a critical step in the formation of hemidesmosomes. An important interaction between these two proteins occurs between the actin-binding domain (ABD) of plectin and the first pair of fibronectin type III (FNIII) domains and a small part of the connecting segment of β4. Previously, a few amino acids, critical for this interaction, were identified in both plectin and β4 and mapped on the crystal structures of the ABD of plectin and the first pair of FNIII domains of β4. In the present study, we used this biochemical information and protein-protein docking calculations to construct a model of the binary complex between these two protein domains. The top scoring computational model predicts that the calponin-homology 1 (CH1) domain of the ABD associates with the first and the second FNIII domains of β4. Our mutational analysis of the residues at the proposed interface of both the FNIII and the CH1 domains is in agreement with the suggested interaction model. Computational simulations to predict protein motions suggest that the exact model of FNIII and plectin CH1 interaction might well differ in detail from the suggested model due to the conformational plasticity of the FNIII domains, which might lead to a closely related but different mode of interaction with the plectin-ABD. Furthermore, we show that Ser-1325 in the connecting segment of β4 appears to be essential for the recruitment of plectin into hemidesmosomes *in vivo*. This is consistent with the proposed model and previously published mutational data. In conclusion, our data support a model in which the CH1 domain of the plectin-ABD associates with the groove between the two FNIII domains of β4.

Several kinds of skin blistering diseases are known to be due to defects in the adhesion of basal cells of the epidermis to the underlying basement membrane. A severe and fatal skin blistering disease called pyloric atresia associated with junctional epidermolysis bullosa (PA-JEB)[1] is caused by the loss of expression of either the α6 or the β4 integrin subunit (1, 2). In addition, missense mutations in the gene encoding β4 have been described in patients with a non-lethal form of epidermolysis bullosa (EB) (3, 4). These mutations (R1225H and R1281W) have been shown to result in a failure of β4 to recruit the intermediate filament linker protein plectin into the epithelial adhesive superstructures called hemidesmosomes (5). Similarly, the loss or a reduced expression of plectin results in a skin blistering disorder called epidermolysis bullosa simplex associated with muscular dystrophy. This further confirms the importance of the interaction of α6β4 with plectin in maintaining epithelial integrity (6–9).

Hemidesmosomes are protein complexes that mediate the stable anchoring of basal cells to the basement membrane in epithelial tissues (10). Two types of hemidesmosomes can be distinguished, type I and type II. Type I hemidesmosomes are present in squamous and complex epithelia and have a complex ultrastructure consisting of an inner and outer dense plaque, separated by an electron-lucent region. They contain at least six distinct proteins: the two subunits of the integrin α6β4 (11–13), plectin (6, 14), the bullous pemphigoid antigens BP180 (15) and BP230 (16), and the tetraspanin CD151 (17). Type II hemidesmosomes are present in simple epithelia, such as that of the gut, and consist of clusters of α6β4 bound to its substrate laminin-5, plectin, and possibly CD151. These less complex hemidesmosomes demonstrate the importance of the interaction of plectin with β4 in the assembly of hemidesmosomes. Indeed, studies with cultured keratinocytes have shown that the incorporation of BP180 and BP230 into hemidesmosomes requires the prior recruitment of plectin by α6β4 (18, 19).

Plectin binds to β4 via its N-terminal actin-binding domain (ABD), and as a result, the association of the ABD with F-actin is prevented (20, 21). The plectin-ABD has previously been shown to interact with the first pair of fibronectin type III (FNIII) domains of β4 (20, 21). However, the resulting association is not sufficient for efficient recruitment of plectin into hemidesmosomes. Additional interactions of the plectin plakin domain with sites in the connecting segment (CS) and C-tail of β4 must occur to stabilize the association and to enable plectin to be recruited into hemidesmosomes (19). The crystal structures of both the plectin-ABD and the first pair of FNIII do-

[1] The abbreviations used are: PA-JEB, pyloric atresia associated with junctional epidermolysis bullosa; EB, epidermolysis bullosa; ABD, actin-binding domain; CH, calponin-homology; CS, connecting segment; FNIII, fibronectin type III; *GAL4*, galactose metabolism regulatory gene; HA, hemagglutinin; IL2R, interleukin-2 receptor.

mains of $\beta4$ have been determined (22–24) but not the structure of the complex of the two proteins.

To predict critical residues of $\beta4$ and the plectin-ABD that are involved in their interaction, we constructed a computational model based on the individual crystal structures by using the 3D-Dock programs (25). One of the top scoring solutions, as suggested by the scoring function implemented in 3D-Dock, satisfied all biochemical information that was available at the time. On the basis of that model, we tested residues on the predicted protein-protein interface through mutagenesis followed by yeast two-hybrid and pull-down assays. This analysis, combined with computational simulations to predict protein-protein motions, confirmed the proposed model. In addition to validating the computational model, we identified Ser-1325 of $\beta4$ (which was not included in the model, as the $\beta4$ crystal structure only comprises residues 1126–1320) as a critical residue necessary for the interaction of $\beta4$ and plectin *in vivo*.

MATERIALS AND METHODS

Construction of a Model for the Plectin-ABD and β4 Complex—We used the crystal structures of plectin (1MB8) and $\beta4$ (1QG3) and the 3D-Dock program suite (25) to construct a theoretical model of their binary complex. The solutions from 3D-Dock were sorted by the residue level pair potential empirical score (RPscore). The final model on which biochemical experiments were based had the third overall RPscore of 5.024 and the second best overall surface complementarity score (SCscore) of 242. In addition, it was compatible with all biochemical data available at that time.

Predictions of Protein Motion—To predict possible motions of the FNIII domains and the plectin-ABD, which could cause conformational alterations that facilitate the binding, we used the Dynamite server (26). In this procedure, the ensemble of possible conformations is created by a non-Newtonian method (27). The trajectory was analyzed with GROMACS (28) to obtain the principal components of predicted protein motions. For the FNIII structure, the three largest eigenvalues were 20.2, 5.1, and 4.8 (and the motions suggested by the corresponding eigenvectors were considered to be significant and are presented), whereas the fourth eigenvalue was 1.51. For the ABD, the first two eigenvalues were 6.1 and 5.2, and the third eigenvalue was 1.6. Motions were visualized with the VMD program (29).

Cell Lines and Antibodies—COS-7 cells were grown in Dulbecco's modified Eagle's medium (Invitrogen) containing 10% fetal bovine serum, 100 units/ml penicillin, and 100 units/ml streptomycin. They were transiently transfected with cDNA constructs by using the DEAE-dextran method (30). The PA-JEB keratinocyte cell lines (31) were maintained in keratinocyte serum-free medium (Invitrogen) supplemented with 50 μg/ml bovine pituitary gland extract, 5 ng/ml epidermal growth factor, 100 units/ml penicillin, and 100 units/ml streptomycin. Stable integration of $\beta4$ integrin mutants was performed as described previously (32).

The rabbit polyclonal antibodies against the extracellular domain of IL2Rα (N-19), the hemagglutinin (HA)-epitope (Y-11), and the extracellular domain of $\beta4$ (H-101), the mouse monoclonal antibodies against the HA-epitope (12CA5), the *GAL4* activation domain, and the *GAL4* DNA-binding domain were purchased from Santa Cruz Biotechnology (Santa Cruz, CA). The mouse monoclonal antibody 450-11A against $\beta4$ was purchased from Pharmingen. Donkey anti-rabbit and goat anti-mouse horseradish peroxidase-conjugated antibodies were purchased from Amersham Biosciences. Fluorescein isothiocyanate-conjugated goat anti-mouse antiserum was obtained from Rockland (Gilbertsville, PA), and goat anti-rabbit Texas Red-conjugated antibodies were obtained from Molecular Probes (Eugene, OR).

cDNA Constructs—The *GAL4* fusion plasmids used in this study are depicted in Figs. 2*A*, 3 (*A* and *D*), and 4*A*. The construction of $\beta4^{1115–1355}$, fused in-frame to the *GAL4* activation domain of the pACT2 vector (Clontech, Palo Alto, CA), and of plectin-1C$^{1–339}$, fused in-frame to the *GAL4* DNA-binding domain of the pAS2.1 vector (Clontech), has been described previously (20). The various point mutants were generated by the PCR overlap extension method.

Plectin-1C$^{1–339}$ in pcDNA3-HA and the IL2R/$\beta4^{cyto}$ chimera have been described previously (20, 33). To construct the plectin-1C$^{1–339}$ mutants in pcDNA3-HA, the plectin mutants in pAS2.1 were amplified using an upstream primer containing an EcoRV restriction site and a downstream primer in plectin containing the EcoRV restriction site at

position 526 of the plectin-1C cDNA. These fragments were exchanged with the EcoRV fragment of wild-type plectin-1C$^{1–339}$ in pcDNA3-HA. To construct the IL2R/$\beta4$ mutants in pCMV, ScaI-BssHII fragments were isolated from the $\beta4^{1115–1355}$ mutants in pACT2, and together with a wild-type BglII-ScaI $\beta4$ fragment, exchanged with the BglII-BssHII fragment of wild-type IL2R/$\beta4$ in pCMV. The plectin-1C CH1/dystrophin CH2 chimera in pAS2.1 was generated by ligation of two separate fragments into pAS2.1. The first fragment (CH1 domain of plectin-1C) was obtained by digestion of plectin-1C$^{1–339}$ with BstXI and subsequent blunt ending with T4 DNA polymerase without the addition of dNTPs followed by digestion with NdeI. The second fragment (CH2 dystrophin) was obtained by PCR using forward oligonucleotides 5′-GTAAATAT-CATGGCTGGGGATTGCAACA-AACC-3′ (sense) and 5′-CCGCGTC-GACGGACTCTCCATCAATGAACTGCC-3′ (antisense) containing a SalI site.

pLZRS-$\beta4^{S1325A}$ and pLZRS-$\beta4^{S1325E}$ were obtained by cloning $\beta4$ cDNA fragments derived by site-directed mutagenesis into the retroviral vector pLZRS-IRES-zeo (17). All PCR fragments were generated by using the proofreading *Pwo* DNA polymerase (Roche Applied Science). All plasmids were verified by sequencing, and protein expression and size were confirmed by Western blotting.

Yeast Two-hybrid Assay—Yeast strain *Saccharomyces cerevisiae* PJ69-4A (a gift from Dr. P. James, University of Wisconsin, Madison, WI), containing the genetic markers *trp1-901*, *leu2-3*, *his3-200*, *gal4Δ*, *gal80Δ*, *LYS2::GAL1-HIS3*, and *GAL2-ADE2* (34), was used as the host for the two-hybrid assay. The use of PJ69-4A was essentially as described previously (20, 31). As a quantitative method to measure the strength of interactions, we used a yeast β-galactosidase assay kit (Pierce), as described by the manufacturer. 3×5 yeast colonies of each transformation were measured in triplicate.

In Vitro Binding Assay and Immunoblotting—COS-7 cells were transiently transfected with wild-type IL2R/$\beta4$ chimera and different plectin-HA-tagged ABD constructs, or alternatively, with wild-type HA-tagged plectin-ABD and different IL2R/$\beta4$ chimera mutants. Lysis of the cells, immunoprecipitation with monoclonal antibody 12CA5, and immunoblotting were performed as described (21).

In Vivo Phosphopeptide Mapping Experiments—PA-JEB cells were phosphate-starved for 1 h. 2 mCi of [^{32}P]orthophosphate was then added to the cells and incubated for an additional 3 h. Calyculin A (Cell Signaling, Inc., Beverly, MA) was added at a final concentration of 100 nM for 15 min at 37 °C. $\beta4$ was isolated with the monoclonal antibody 450-11A as described above. The entire sample was loaded onto an SDS-PAGE gel, run, and then dried. The film was exposed for 3 h at room temperature. The radioactive $\beta4$ bands were then isolated and digested with trypsin, and phosphopeptide mapping was performed as described previously (35, 36).

RESULTS

Computational Model of the Complex of the Plectin-ABD with β4—Since the complex of plectin with $\beta4$ has not been crystallized, we used the separate crystal structures of plectin (1MB8) and $\beta4$ (1QG3) and the 3D-Dock program suite (25) to construct possible models of their binary complex. The best documented biochemical data available suggested that Asn-149 of plectin and Arg-1225 and Arg-1281 of $\beta4$ are essential for their interaction (5, 21). From the 3D-Dock solutions scored by the residue level pair potential empirical score (RPscore), we first selected those that satisfied a criterion for proximity of Asn-149 to $\beta4$ residues. After filtering the list of solutions for proximity of Arg-1281 to plectin, most top RPscore ranking solutions were maintained. Filtering for proximity of Arg-1225 eliminated the top ranking solutions. Filtering the initial list of solutions with either Asn-149 or Arg-1281 alone, or with the two together, the same top ranking solution was selected. Notably, this solution had the third overall RPscore (5.024) and the second best overall surface complementarity score (SCscore, 242). Thus we decided to examine that model manually, ignoring the criterion for proximity of Arg-1225. It became immediately obvious that the side chain of Arg-1225 of $\beta4$ could easily adopt a conformation that would allow interaction with plectin residues. Given the relatively high atomic displacement factor (B value) for the Arg-1225 atoms (between 26 and 31 Å^2, as compared with an overall B value from the Wilson plot of around 14) and the lack

Fig. 1. **A schematic representation of a general view of the complex between the first two β4 FNIII repeats and the plectin-ABD.** *A*, the two FNIII repeats are in *cyan*, the CH1 of the ABD is in *magenta*, and the CH2 is in *red*. The residues discussed in the text are drawn as *stick models*. All nitrogens are *bright blue*, and oxygens are *bright red*, whereas the carbon atoms are: *yellow* for the residues known to be important for binding and were used as anchor points in docking; *orange* for residues that were known to be important for binding, were not used as anchor points in docking, but gave initial indications that the docking was correct; *green* for residues mutated in the present study; their mutation abrogated binding, and thus they directly confirm the model; *dark red* for residues mutated in the present study but that do not confirm the model; and *dark blue* for residues that were mutated in the present study or previously and had no effect on binding, thus confirming the model indirectly. N and C termini as well as important secondary structure elements are labeled. *B*, a stereo view of the proposed binding interface, in a view close to the one in *panel A*. The color scheme is identical to the latter panel, but all residues are now also labeled. *C*, a schematic representation of suggested relative protein motions of the FNIII domains. The *orange arrows* indicate the suggested rotations, whereas the approximate rotation axes are in *black*. *D*, a suggested mode of binding of the CS to the CH2 or CH1 domains of plectin.
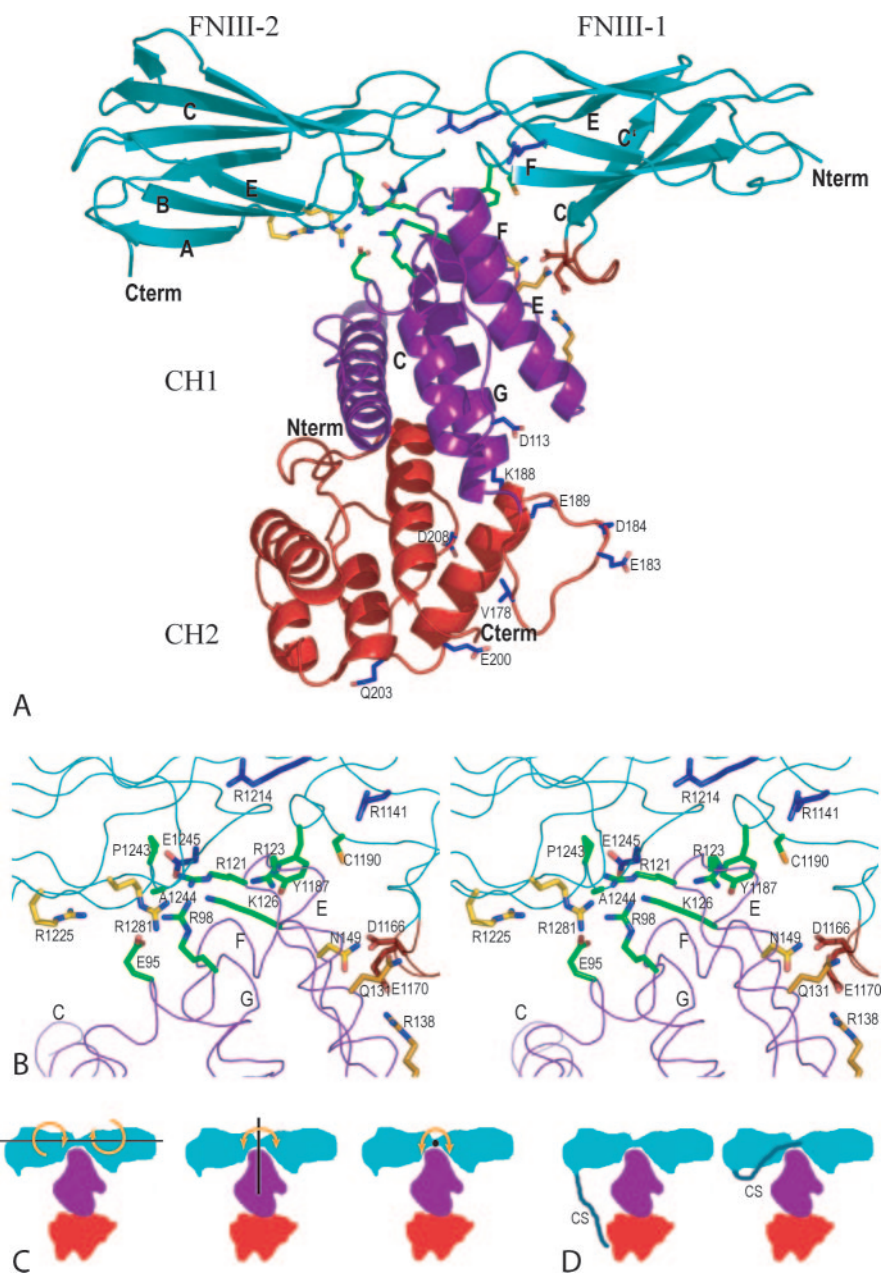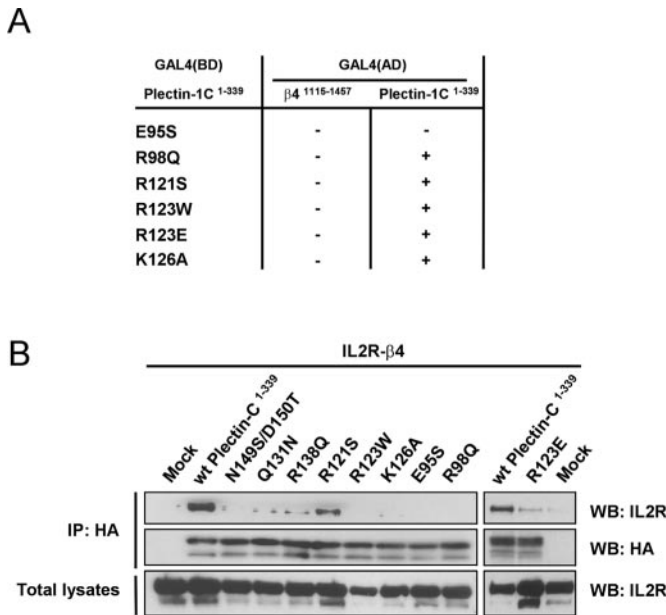

of specific interactions with any other atoms in the β4 structure, it is very likely that this residue can indeed adopt alternative conformations and interact with plectin, whereas the overall model is preserved. Thus we decided to use that model (shown in Fig. 1*A*) as a guide to further predict residues that are likely to be involved in the β4-plectin interaction. The region of β4 predicted to interact with the plectin-ABD extends over an interdomain region that includes the C-C′ and E-F loops in the first FNIII and the lower part of the ABE sheet and the B-C loop of the second FNIII domain. Furthermore, the CH1 domain, but not the CH2 domain, of the plectin-ABD was predicted to be involved in direct binding to this interdomain region of β4. The region of the CH1 domain of plectin predicted to bind to β4 contains helices E and F and the loop preceding helix C, which is in close proximity to helix E. Apart from Asn-149 in plectin and Arg-1225 and Arg-1281 in β4, Gln-131 and Arg-138 in plectin had previously been reported to be important for the interaction with β4, whereas Asp-135 was shown not to be essential for binding (21). Indeed, Asp-135 was not predicted to be involved in the binding, and Gln-131

was calculated to interact with Asp-1166 in β4 (Fig. 1*B*). However, in our model, Arg-138 was not shown to be close to any of the residues in β4. It was, however, possible that the Glu-1170 in β4 could adopt a conformation that would allow the formation of a salt bridge with Arg-138, and thus Glu-1170 was chosen as a putative binding partner of Arg-138 in plectin. The model also confirms that the amino acids of the plectin-ABD, which were shown not to be required for binding to β4 in yeast two-hybrid assays (Asp-113, Val-178, Glu-183, Glu-184, Lys-188, Glu-189, Glu-200, Gln-203, Asp-208) are indeed not essential.[2]

Verification of the Critical Residues in the Binding Sites on Plectin—Based on the predicted interactions between amino acids, we generated plectin mutants that were tested in a yeast two-hybrid assay (Fig. 2*A*). The amino acids in plectin were replaced by the corresponding amino acids in the dystrophin-ABD, which does not bind to β4 (20, 21). Each single point

---

[2] S. H. M. Litjens, unpublished results.

A

GAL4(BD)	GAL4(AD)	
Plectin-1C [1-339]	β4 [1115-1457]	Plectin-1C [1-339]
E95S	−	−
R98Q	−	+
R121S	−	+
R123W	−	+
R123E	−	+
K126A	−	+

B

FIG. 2. **Verification of the plectin-binding surface.** Binding of the plectin-ABD mutants to wild-type (*wt*) β4 and wild-type plectin-ABD in yeast two-hybrid assays (*A*) or to IL2R-β4 in pull-down assays (*B*). (+) scoring of the interaction in A indicates plating efficiencies on selective plates greater than 80% of those on non-selective plates at 5 days of growth. (−) scoring indicates no colonies after 10 days of growth. *IP*, immunoprecipitation; *WB*, Western blot.

mutation of the indicated amino acids (E95S, R98Q, R121S, R123W, R123E, and K126A) completely abrogated the binding of the plectin-ABD to β4 in yeast two-hybrid assays. Arg-123, which is conserved in plectin and dystrophin, was replaced by a tryptophan to introduce a bulky side chain or by a glutamic acid to introduce an opposite charge. These two mutations had the same effect, *i.e.* they abrogated binding to β4. It is unlikely that the loss of binding is a result of destruction of the structure of the ABD since all mutants, except E95S, were still able to form dimers with the wild-type plectin-ABD (Fig. 2*A*) (37). Since the expression of the plectin[E95S]-ABD mutant could be confirmed in yeast, its size was as expected, and Glu-95 is highly exposed to the solvent, this residue is probably important for the dimerization of the ABD, rather than critical for its correct folding. The yeast two-hybrid results were confirmed by pull-down assays using HA-tagged plectin mutants and the IL2R/β4[cyto] chimera, as described previously (21). As shown in Fig. 2*B*, almost all of the plectin-ABD mutants did not at all bind, or only very poorly bound, to the IL2R-β4 chimera. The plectin[R121S]-ABD mutant however, showed clear binding activity toward the IL2R/β4[cyto] chimera but much less than the wild-type plectin-ABD. These findings confirm that combining the model constructed by the 3D-Dock program together with the initial biochemical data correctly predicts the critical residues in the binding surface on the plectin-ABD molecule.

Verification of the Critical Residues in the Binding Sites on β4—Based on the predicted interactions, we generated β4 mutants and tested them in a yeast two-hybrid assay (D1166W, E1170W, Y1187W, P1243W, A1244W, and E1245W; Fig. 3*A*). We chose to initially replace all these amino acids by a bulky tryptophan residue, to create as much "steric expulsion" as possible while eliminating available hydrogen bond donors and acceptors. Since not all of these mutations in β4 abrogated the binding to the plectin-ABD in yeast two-hybrid assays, which were quantified using a β-galactosidase assay (Fig. 3*B*), we opted for a second round of mutations (loop 1164QGD-SESE1170 in the first FNIII domain was replaced by amino acids 1260VNDDNRPIGP1269 of the complementary loop in

the second FNIII domain, Y1187R/C1190R, R1141E, and R1214E) to further test our hypothesis (Fig. 3*D*). Because the interdomain orientation of the two FNIII domains may be flexible, mutations were generated in all three loops and the linker between the two FNIII domains. The results of the yeast two-hybrid assays were confirmed in pull-down assays using a wild-type HA-tagged plectin-ABD and mutants of the IL2R/β4[cyto] chimera (Fig. 3, *C* and *D*). Replacement of Pro-1243 and Ala-1244 in β4 resulted in a complete and significant loss of binding to plectin, respectively. Substitution of Glu-1245 had no effect on the binding. However, although it lies next to Ala-1244, this residue points away from the interface in the suggested model. Mutation of Glu-1170 did not affect binding, but the hypothesis that Glu-1170 is involved in the binding to plectin Arg-138 was not directly suggested by the model (see above). Substitution of Tyr-1187 by tryptophan did not result in loss of binding, but we suggest that it maintained a hydrophobic contact of the aromatic ring with Arg-123 of the plectin-ABD. Therefore, Tyr-1187 was mutated to arginine, along with the neighboring Cys-1190, which together bracket the EF loop. In support for our hypothesis, the Y1187R/C1190R mutant was unable to bind plectin. Mutation of Asp-1166, predicted to interact with Asn-149 and Gln-131 in the plectin-ABD, or substitution of the whole 1164–1170 loop had only little effect on the binding. The replacement of Asp-1166 by tryptophan is expected to induce important changes in the β4 surface, and the fact that it does not influence the binding of β4 to the plectin-ABD implies that Asp-1166 is not involved in the direct binding to the plectin-ABD. Moreover, the fact that substitution of the whole CC′ loop to which Asp-1166 belongs has no profound effect on binding confirms the idea that this loop does not make crucial contacts with the plectin-ABD. Substitution of Arg-1141 in the AB loop and Arg-1214 in the G2 β-strand preceding the linker between the two FNIII domains to glutamic acids had no effect on binding, which is in support of our model.

Our data collectively suggest that although some conformational flexibility and deviations from the proposed model are likely, they should not be significant enough to bring totally different surface areas of the FNIII domains in contact with the plectin ABD. Probably, conformational flexibility of the two FNIII domains allows them to adopt different orientations in solution, one of which is "frozen" in the crystal structure. Alternatively, their relative orientation may be different in the full-length protein, or there may be an induced fit upon complex formation with the plectin-ABD. In summary, our results indicate that the EF loop of the first FNIII domain that contains Tyr-1187 and Cys-1190 and the BC loop of the second FNIII domain that contains the amino acids Pro-1243 and Ala-1244 are important for the interaction with the plectin-ABD.

Predictions of Protein Motion—To support the idea that the relative orientation of the two FNIII domains may vary, we performed computational simulations of protein dynamics. Two opposing "screw" movements of each domain along the long interdomain axis compose the major motion between the two FNIII domains (Fig. 1*C*, *left picture*). Such a movement, even if small, can dramatically change the area that is available for complex formation. This provides an excellent explanation for our biochemical findings showing that the interacting residues of the second FNIII domain of β4 were predicted correctly but that the prediction of residues of the first FNIII domain was only partially correct. A small rearrangement, such as the movement along the interdomain axis, might lead to the presentation of different residues on the first FNIII domain for binding to the plectin-ABD. The two other predicted major
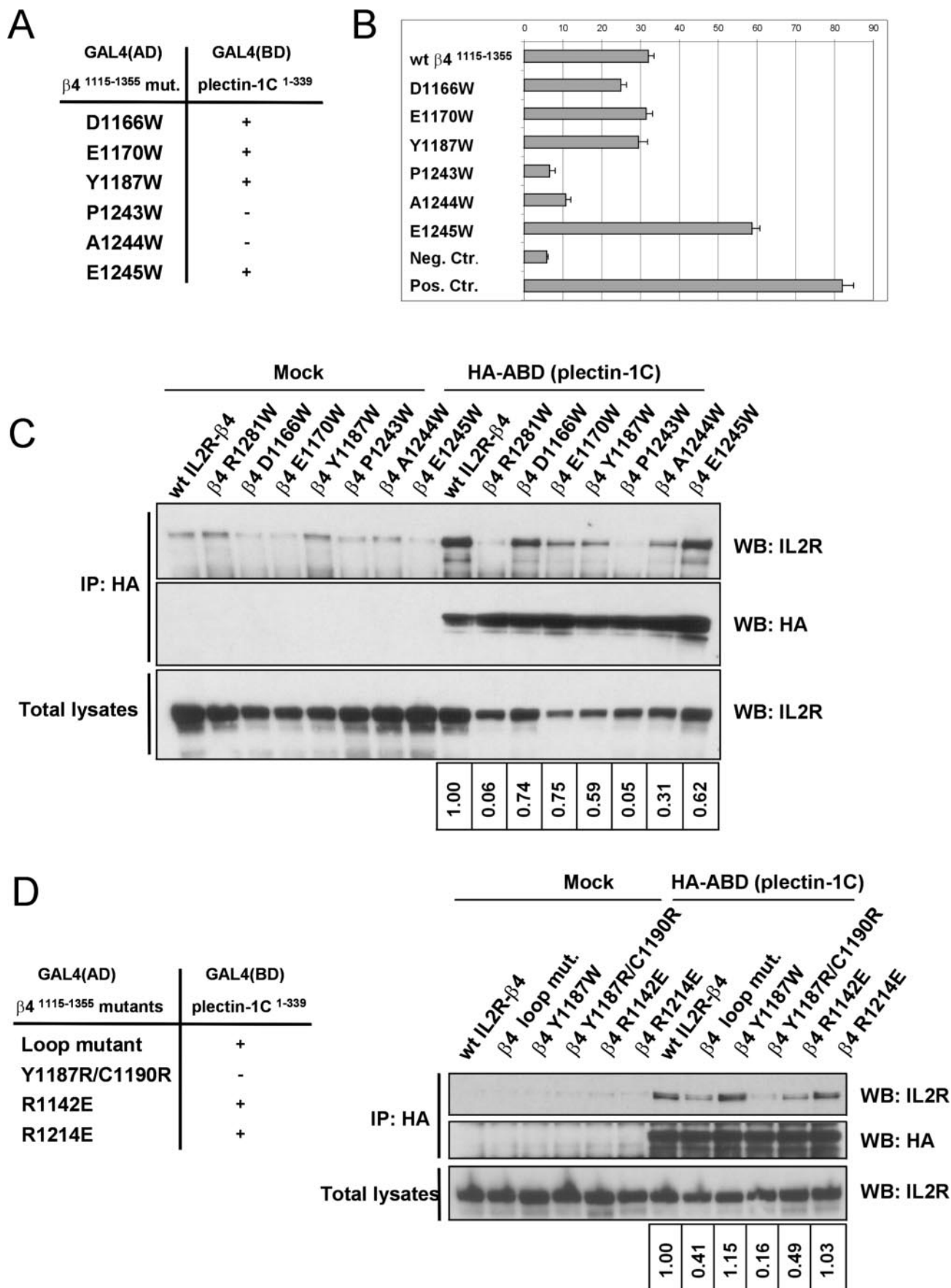
Plectin-β4 Docking Model

A

GAL4(AD)	GAL4(BD)
β4 $^{1115\text{-}1355}$ mut.	plectin-1C $^{1\text{-}339}$
D1166W	+
E1170W	+
Y1187W	+
P1243W	−
A1244W	−
E1245W	+

B

C

1.00	0.06	0.74	0.75	0.59	0.05	0.31	0.62

D

GAL4(AD)	GAL4(BD)
β4 $^{1115\text{-}1355}$ mutants	plectin-1C $^{1\text{-}339}$
Loop mutant	+
Y1187R/C1190R	−
R1142E	+
R1214E	+

1.00	0.41	1.15	0.16	0.49	1.03

FIG. 3. **Verification of the β4-binding surface.** Binding of the β4 mutants (*mut.*) to wild-type (*wt*) plectin-ABD in yeast two-hybrid assays (*A*, *B*, and *D*) and in pull-down assays (*C* and *D*). (+) scoring of the interaction in *A* and *D* indicates plating efficiencies greater than 70% at 5 days of growth. (−) scoring indicates no colonies at 5 days of growth or an efficiency of less than 10% at 10 days of growth. The values representing the quantitative β-galactosidase assay (*B*) are arbitrary and representatives of multiple assays. The negative control (*Neg. Ctr.*) is represented by the
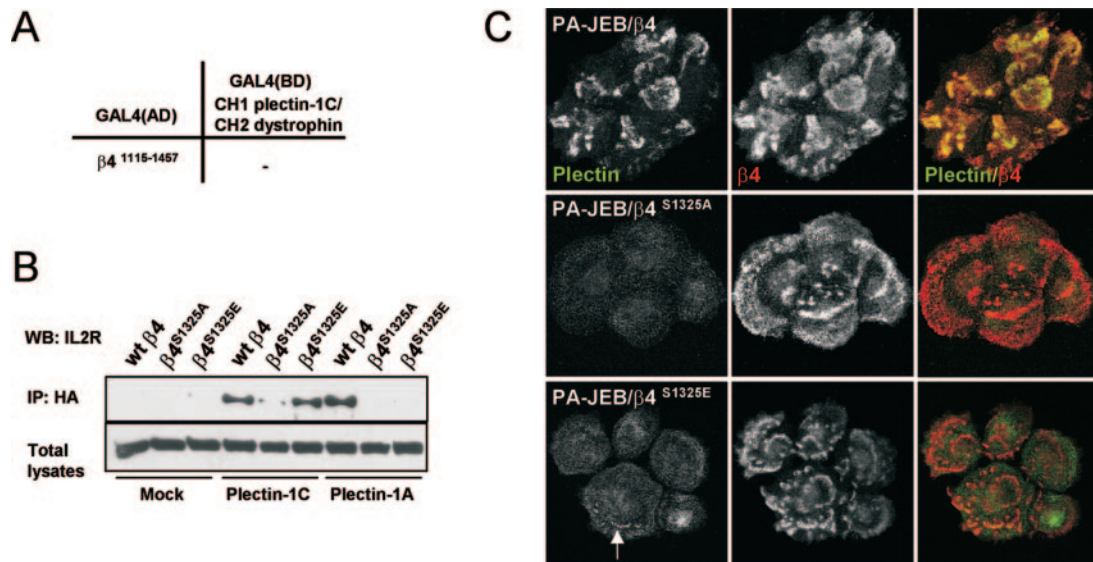
FIG. 4. **Role of the CH2 domain of plectin and the CS of β4.** *A*, yeast two-hybrid analysis of the interaction between β4 and a plectin-1C CH1/dystrophin CH2 chimera. *B*, biochemical analysis of the interaction between plectin-ABD and β4[S1325A/E] mutants. *WB*, Western blot; *IP*, immunoprecipitation; *wt*, wild type. *C*, recruitment of plectin into hemidesmosomes by β4[S1325A/E] mutants in PA-JEB/β4 cells. PA-JEB/β4, PA-JEB/β4[S1325A] and PA-JEB/β4[S1325E] cells were stained for β4 (*red*) and plectin (*green*). Colocalization appears as *yellow*.

motions correspond to two orthonormal "bending" motions of the region between the two FNIII domains (Fig. 1*C*, *middle* and *right pictures*), which would also lead to the presentation of other residues for plectin binding. The predicted motions for the plectin-ABD, which change the relative orientation of the CH1 and CH2 domains, are minor and do not allow any further significant conclusions (not shown).

Role of the CH2 Domain of Plectin, the Sequence Preceding the Plectin-ABD, and the Connecting Segment of β4—The predicted model does not implicate the CH2 domain of plectin in the association with β4. Nevertheless, we have shown previously that the presence of the CH2 domain is essential for the interaction with β4 (20). To test the hypothesis that the CH2 domain might be required for the proper folding of the plectin-ABD, we swapped the CH2 domain of plectin with that of dystrophin, which does not bind to β4 (21). We would expect that the chimeric ABD still binds to β4 if the CH2 domain of plectin is only necessary for structural reasons. Binding was tested in a yeast two-hybrid assay (Fig. 4*A*). The CH1 plectin-1C/CH2 dystrophin chimera did not bind to β4, indicating that the correct plectin-CH2 domain is essential for the interaction with β4, either directly or indirectly.

The two crystal structures used for the modeling lack the sequence preceding the ABD of plectin and the CS of β4. However, the sequence preceding the plectin-ABD has been found to be an important modulator of the affinity of this protein for β4 (21). Our model does suggest that this sequence will be in close proximity to the actual binding site (Fig. 1*A*), and therefore, does support the concept that this sequence modulates affinity. Furthermore, the CS of β4 was found to be extremely important for the interaction with plectin. In fact, deletion of 27 amino acids of the CS from position 1328 to 1355 abrogates the ability of β4 to recruit plectin into hemidesmosomes *in vivo* (20, 31). Since the CS was not present in the crystal structure of β4, this part of the actual binding surface between β4 and plectin could not be modeled. However, analogous to the sequence preceding the plectin-ABD, the entire CS of β4 is ideally placed

for interaction with the plectin-ABD (Fig. 1*A*). So both the N-terminal sequence of plectin and the CS of β4 are in close proximity of the binding interface and may therefore regulate this interaction.

Identification of Ser-1325 in the β4 CS as Important Residue for Interaction with Plectin in Vivo—To determine residues present within the CS of β4 that are important for the regulation of the interaction with plectin, we first decided to mutate serine residues that are present in consensus sequences of protein kinases. It is well documented that serine phosphorylation can modulate protein-protein interactions. Ser-1325 is part of a consensus site for phosphorylation by protein kinase A and Cam kinase II and is located in the region that was previously shown to be critical for high affinity binding to β4 (19, 20). To establish whether Ser-1325 is involved in regulating the interaction between the plectin-ABD and β4, we replaced this residue by alanine to prevent phosphorylation and to glutamic acid to mimic phosphorylation. The mutants were tested for plectin binding in pull-down assays and for their ability to recruit plectin into hemidesmosomes (Fig. 4, *B* and *C*). In pull-down assays, binding to plectin-1A was completely lost with the S1325A mutation and completely lost or significantly decreased with the S1325E mutation, depending on the experiment (Fig. 4*B*). On the other hand, only the alanine, but not the glutamic acid mutation, decreased binding to plectin-1C (Fig. 4*B*). This difference in binding of plectin-1A and plectin-1C to the mutants once more indicates the importance of the sequences preceding the plectin-ABD. In addition, both mutations had a strong effect on the recruitment of plectin into hemidesmosomes (Fig. 4*C*). Hardly any endogenous plectin was found in the hemidesmosomes of the PA-JEB/β4[S1325A] or PA-JEB/β4[S1325E] mutant cell lines, which is in agreement with the observation that mainly plectin-1A is present in the hemidesmosomes of keratinocytes (38). These results indicate that Ser-1325 is crucial for the recruitment of plectin into hemidesmosomes. In the very few hemidesmosomes in which plectin was present (Fig. 4*C*, *arrow*), it was possibly recruited by BP180

interaction after cotransfection of plectin-ABD in pAS2.1 and a mock pACT2 vector (*Mock*). The positive control (*Pos. Ctr.*) is represented by the interaction between PTP1-1 and PVA3-1. The values in *C* and *D* indicate the relative strength of the interaction, calculated by determining the percentage of coprecipitated IL2R/β4, as compared with the total IL2R/β4 and correcting this value for the amount of precipitated HA-plectin-ABD. *AD*, activation domain; *BD*, binding domain; *IP*, immunoprecipitation; *WB*, Western blot.
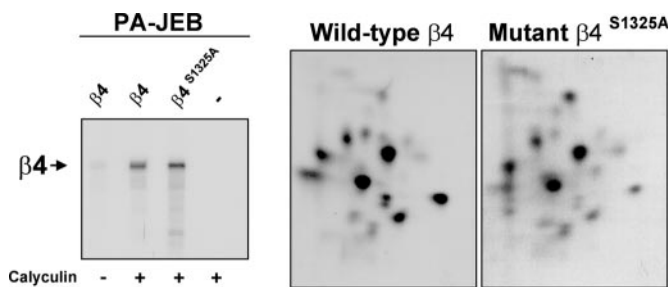
Plectin-β4 Docking Model

FIG. 5. *In vivo* **phosphopeptide mapping of wild-type and mutant β4**$^{\text{S1325A}}$**.** PA-JEB or PA-JEB cells expressing either wild-type β4 or β4$^{\text{S1325A}}$ were treated with 100 nM calyculin A for 15 min at 37 °C in the presence of 2 mCi of [^{32}P]orthophosphate. β4 was isolated by immunoprecipitation, and samples were run on an SDS-PAGE gel. The dried gel was exposed to film for 3 h at room temperature (*left panel*). The calyculin A-treated samples were isolated from the gel and subjected to phosphopeptide mapping, as described under "Materials and Methods" (*right panels*).

and/or BP230.

The fact that both the alanine and glutamic acid mutants had similar effects *in vivo* suggests that either glutamic acid does not mimic a phosphorylated serine residue in this case or Ser-1325 is not a phosphorylation site. To further investigate this, we stimulated PA-JEB keratinocytes, expressing the S1325A mutant or wild-type β4, with calyculin A in the presence of [^{32}P]orthophosphate and subjected the phosphorylated β4 subunit to phosphopeptide mapping analysis (Fig. 5). Calyculin A inhibits the serine/threonine phosphatases PP1 and PP2A, which results in an increase in the phosphorylation of serine and threonine on proteins (39, 40). We saw no phosphopeptides disappear in the β4$^{\text{S1325A}}$ mutant map, indicating that Ser-1325 is not an *in vivo* phosphorylation site (Fig. 5, *right panels*). However, we cannot rule out the possibility that an as yet unidentified phosphatase, which is not inhibited by calyculin A, is responsible for the regulation of phosphorylation at this site. Nevertheless, in addition, comparison of phosphopeptide maps of wild-type β4 and β4$^{\text{S1325A}}$, *in vitro* phosphorylated with protein kinase A, did not reveal significant changes in phosphorylation of any of the peptides. Together, these findings indicate that sequences that are not present in the crystal structures do have a major impact on the binding of β4 to plectin, consistent with previously published data (19).

DISCUSSION

In this study, we have used a model obtained by computational modeling of protein-protein interactions assisted by biochemical data to predict which residues are involved in the interaction between the plectin-ABD and the first pair of FNIII domains of β4. We have validated this model by mutagenesis experiments.

It was correctly predicted which amino acids on the plectin-ABD are involved in the binding to β4, *i.e.* the CH1 domain of the plectin-ABD is clearly involved in this binding. The model did not predict that the CH2 domain binds directly to β4. However, deletion or replacement of the CH2 domain by the CH2 domain from another ABD, which is known not to interact with β4, abolishes interaction with β4, suggesting that the CH2 domain at least contributes to the binding. The CH2 domain might interact directly with sequences of β4 that are not present in the crystal structure, such as the CS. Indeed, the position of the CS is such that it might interact with the CH2 domain of the ABD (further discussed below). Alternatively, the CH2 domain might be indirectly involved in the interaction by correctly folding and positioning the CH1 domain for interaction with the two FNIII domains.

The predicted binding surface on β4 appears to be largely

correct, but not entirely. In agreement with our model, the EF loop of the first FNIII domain, containing amino acids Tyr-1187 and Cys-1190, and the BC loop of the second FNIII domain, containing amino acids Pro-1243 and Ala-1244, are clearly vital for the interaction with plectin. However, the CC' loop in the first FNIII domain that was predicted to be involved in the interaction is clearly not essential. One explanation for this could be that the CC' loop is on the outside of the interface and can be "pushed away" without affecting binding. This hypothesis, however, is not fully satisfactory because this would mean that Asn-149 of the plectin-ABD is not crucial for binding, whereas it was actually shown to be so (21). In the second FNIII domain, Pro-1243 is mostly buried under the BC loop. Therefore, the mutation P1243W is likely to create a distortion affecting the whole loop, reinforcing the importance of this entire loop for the binding to the plectin-ABD. Replacement of Glu-1245 by tryptophan does not abrogate binding. This does not actually contradict the model since Glu-1245 is oriented away from the interface and the tryptophan substitution could therefore be tolerated at that position.

In an attempt to provide possible explanations for the fact that our biochemical data do not fully validate the model, we performed a protein motion prediction computational experiment. Those data support the idea that there is conformational freedom of the two FNIII domains, which could explain why the binding interface between β4 and plectin is different from that suggested by the model. Interestingly, a recent report showed that the binding of integrins to fibronectin is strongly dependent on the interdomain tilt between the ninth and tenth FNIII domains of fibronectin (41). Furthermore, the flexibility in our model might be combined with an induced fit of the FNIII domain structure upon binding to the plectin-ABD. Indeed, there is an example of a pair of FNIII domains from the human growth hormone-binding protein (hGHbp), which show a bent structure when bound to ligand (42). However, since the structure of the human growth hormone-binding protein when it is not bound to its ligand is not known, we have no strong arguments to support the assumption of an induced fit. Finally, the relative orientation of the two domains in the crystal structure may be different from that in the full-length protein. Whatever the exact explanation, it is likely that a new binding site for the plectin-ABD is exposed on the first FNIII domain when it binds to plectin, whereas the binding surface on the second FNIII domain is maintained. Furthermore, as we have shown previously, the plectin-ABD can form dimers (37), which was not taken into account while modeling the plectin-β4 complex. Although measurement of the interaction between β4 and the plectin-ABD in solution by isothermal titration calorimetry suggests that binding of β4 to the plectin-ABD occurs in a one-to-one stoichiometry (22), dimerization of the ABD might affect the binding interface. Lastly, it should be noted that the plectin-ABD can adopt an open or a closed conformation. Binding to β4 occurs when its conformation is closed as in the crystal structure used (22).

In this study, we also show that Ser-1325 in the CS of β4 (which is not included in the model) is critical for the interaction between the plectin-ABD and β4. This is consistent with previously published data from our laboratory, which showed that other residues in the CS, Pro-1330 and Pro-1333, are also important for the interaction (19). We have two hypotheses for the binding of the CS of β4 to the plectin-ABD. Firstly, the CS might bind to the CH2 domain of plectin, thereby confirming the importance of the CH2 domain in direct binding. Indeed, the last residue in the structure of β4, Pro-1320, is oriented in such a way that the following sequence projects from the FNIII domain in a direction optimal for contacting the helices E and

F and the EF loop of the CH2 domain (Fig. 1, *A* and *D*, *left panel*). Moreover, mutations in other regions of the CH2 domain did not have an effect on binding to β4 (Fig. 1*A*). In this model, the residue Ser-1325 may make direct contact with the CH2 domain of the plectin-ABD. Alternatively, due to the many proline residues in the region 1320–1355 of the CS, this part of CS may fold back onto the second FNIII domain of β4, allowing Ser-1325 to directly contact the CH1 domain of the plectin-ABD (Fig. 1*D*, *right panel*). Indeed, preliminary results indicate that the second hypothesis, *i.e.* the CS binding to the CH1 domain of plectin, is most likely the correct one.[3]

Although we identified Ser-1325 as a putative phosphorylation site for protein kinase A or Cam kinase II, the importance of Ser-1325 for binding to the plectin-ABD appears to be independent of phosphorylation. Using phosphopeptide mapping, we could not prove that Ser-1325 is phosphorylated *in vivo*. However, it is worth noting that we consistently saw that the intensity of several phosphopeptides in the S1325A maps had decreased as compared with that of the corresponding peptides in the wild-type maps. It is possible that the S1325A mutation somehow disrupts the β4 structure, thereby decreasing the accessibility of these phosphorylation sites for kinases. It is equally possible that Ser-1325 actually is a phosphorylation site but that due to the presence of additional phosphorylation sites on the mutated tryptic peptide, the effects of the mutation on the phosphorylation of Ser-1325 become masked. However, the migration of the lower intensity peptides is not significantly different from that of the same phosphopeptides in the wild-type β4 map, as would be expected if a charged phosphate group is replaced by a more hydrophobic alanine. In addition, in the phosphopeptide maps of wild-type β4 and β4[S1325A], *in vitro* phosphorylated with protein kinase A, we saw no obvious tryptic peptides that could possibly contain a phosphorylated Ser-1325 (data not shown). These results together suggest that Ser-1325 is not a phosphorylation site but that, nevertheless, the residue is clearly necessary for the interaction of β4 with plectin in cells.

REFERENCES

1. Vidal, F., Aberdam, D., Miquel, C., Christiano, A. M., Pulkkinen, L., Uitto, J., Ortonne, J. P., and Meneguzzi, G. (1995) *Nat. Genet.* **10,** 229–234
2. Ruzzi, L., Gagnoux-Palacios, L., Pinola, M., Belli, S., Meneguzzi, G., D'Alessio, M., and Zambruno, G. (1997) *J. Clin. Investig.* **99,** 2826–2831
3. Pulkkinen, L., Rouan, F., Bruckner-Tuderman, L., Wallerstein, R., Garzon, M., Brown, T., Smith, L., Carter, W., and Uitto, J. (1998) *Am. J. Hum. Genet.* **63,** 1376–1387
4. Nakano, A., Pulkkinen, L., Murrell, D., Rico, J., Lucky, A. W., Garzon, M., Stevens, C. A., Robertson, S., Pfendner, E., and Uitto, J. (2001) *Pediatr. Res.* **49,** 618–626
5. Koster, J., Kuikman, I., Kreft, M., and Sonnenberg, A. (2001) *J. Investig. Dermatol.* **117,** 1405–1411
6. Gache, Y., Chavanas, S., Lacour, J. P., Wiche, G., Owaribe, K., Meneguzzi, G., and Ortonne, J. P. (1996) *J. Clin. Investig.* **97,** 2289–2298
7. McLean, W. H., Pulkkinen, L., Smith, F. J., Rugg, E. L., Lane, E. B., Bullrich, F., Burgeson, R. E., Amano, S., Hudson, D. L., Owaribe, K., McGrath, J. A., McMillan, J. R., Eady, R. A., Leigh, I. M., Christiano, A. M., and Uitto, J. (1996) *Genes Dev.* **10,** 1724–1735
8. Smith, F. J., Eady, R. A., Leigh, I. M., McMillan, J. R., Rugg, E. L., Kelsell, D. P., Bryant, S. P., Spurr, N. K., Geddes, J. F., Kirtschig, G., Milana, G., de Bono, A. G., Owaribe, K., Wiche, G., Pulkkinen, L., Uitto, J., McLean, W. H., and Lane, E. B. (1996) *Nat. Genet.* **13,** 450–457
9. Andrä, K., Lassmann, H., Bittner, R., Shorny, S., Fassler, R., Propst, F., and Wiche, G. (1997) *Genes Dev.* **11,** 3143–3156
10. Koster, J., Borradori, L., and Sonnenberg, A. (2004) *Handbook of Experimental Pharmacology: Volume Cell Adhesion*, pp. 243–280, Springer-Verlag Gmbh & Co. KG, Berlin-Heidelberg
11. Stepp, M. A., Spurr-Michaud, S., Tisdale, A., Elwell, J., and Gipson, I. K. (1990) *Proc. Natl. Acad. Sci. U. S. A.* **87,** 8970–8974
12. Sonnenberg, A., Calafat, J., Janssen, H., Daams, H., van der Raaij-Helmer LM, Falcioni, R., Kennel, S. J., Aplin, J. D., Baker, J., Loizidou, M., and Garrod, D. (1991) *J. Cell Biol.* **113,** 907–917
13. Jones, J. C., Kurpakus, M. A., Cooper, H. M., and Quaranta, V. (1991) *Cell Regul.* **2,** 427–438
14. Hieda, Y., Nishizawa, Y., Uematsu, J., and Owaribe, K. (1992) *J. Cell Biol.* **116,** 1497–1506
15. Giudice, G. J., Emery, D. J., and Diaz, L. A. (1992) *J. Investig. Dermatol.* **99,** 243–250
16. Skalli, O., Jones, J. C., Gagescu, R., and Goldman, R. D. (1994) *J. Cell Biol.* **125,** 159–170
17. Sterk, L. M., Geuijen, C. A., Oomen, L. C., Calafat, J., Janssen, H., and Sonnenberg, A. (2000) *J. Cell Biol.* **149,** 969–982
18. Koster, J., Geerts, D., Favre, B., Borradori, L., and Sonnenberg, A. (2003) *J. Cell Sci.* **116,** 387–399
19. Koster, J., van Wilpe, S., Kuikman, I., Litjens, S. H. M., and Sonnenberg, A. (2004) *Mol. Biol. Cell* **15,** 1211–1223
20. Geerts, D., Fontao, L., Nievers, M. G., Schaapveld, R. Q., Purkis, P. E., Wheeler, G. N., Lane, E. B., Leigh, I. M., and Sonnenberg, A. (1999) *J. Cell Biol.* **147,** 417–434
21. Litjens, S. H. M., Koster, J., Kuikman, I., van Wilpe, S., de Pereda, J. M., and Sonnenberg, A. (2003) *Mol. Biol. Cell* **14,** 4039–4050
22. Garcia-Alvarez, B., Bobkov, A., Sonnenberg, A., and de Pereda, J. (2003) *Structure (Camb.)* **11,** 615–625
23. de Pereda, J. M., Wiche, G., and Liddington, R. C. (1999) *EMBO J.* **18,** 4087–4095
24. Sevcik, J., Urbanikova, L., Kost'an, J., Janda, L., and Wiche, G. (2004) *Eur. J. Biochem.* **271,** 1873–1884
25. Gabb, H., Jackson, R., and Sternberg, M. (1997) *J. Mol. Biol.* **272,** 106–120
26. Barrett, C. P., Hall, B. A., and Noble, M. E. (2004) *Acta Crystallogr. Sect. D Biol. Crystallogr.* **60,** 2280–2287
27. de Groot, B. L., van Aalten, D. M., Scheek, R. M., Amadei, A., Vriend, G., and Berendsen, H. J. (1997) *Proteins* **29,** 240–251
28. Lindahl, E., Hess, B., and vd Spoel, D. (2001) *J. Mol. Model.* **7,** 306–317
29. Humphrey, W., Dalke, A., and Schulten, K. (1996) *J. Mol. Graph.* **14,** 33–38
30. Seed, B., and Aruffo, A. (1987) *Proc. Natl. Acad. Sci. U. S. A.* **84,** 3365–3369
31. Schaapveld, R. Q., Borradori, L., Geerts, D., van Leusden, M. R., Kuikman, I., Nievers, M. G., Niessen, C. M., Steenbergen, R. D., Snijders, P. J., and Sonnenberg, A. (1998) *J. Cell Biol.* **142,** 271–284
32. Geuijen, C., and Sonnenberg, A. (2002) *Mol. Biol. Cell* **13,** 3845–3858
33. Nievers, M. G., Schaapveld, R. Q., Oomen, L. C., Fontao, L., Geerts, D., and Sonnenberg, A. (1998) *J. Cell Sci.* **111,** 1659–1672
34. James, P., Halladay, J., and Craig, E. A. (1996) *Genetics* **144,** 1425–1436
35. Wilhelmsen, K., Burkhalter, S., and van der Geer, P. (2002) *Oncogene* **21,** 1079–1089
36. van der Geer, P., and Hunter, T. (1993) *EMBO J.* **12,** 5161–5172
37. Fontao, L., Geerts, D., Kuikman, I., Koster, J., Kramer, D., and Sonnenberg, A. (2001) *J. Cell Sci.* **114,** 2065–2076
38. Andrä, K., Kornacker, I., Jorgl, A., Zorer, M., Spazierer, D., Fuchs, P., Fischer, I., and Wiche, G. (2003) *J. Investig. Dermatol.* **120,** 189–197
39. Resjo, S., Oknianska, A., Zolnierowicz, S., Manganiello, V., and Degerman, E. (1999) *Biochem. J.* **341,** 839–845
40. Ishihara, H., Martin, B. L., Brautigan, D. L., Karaki, H., Ozaki, H., Kato, Y., Fusetani, N., Watabe, S., Hashimoto, K., Uemura, D., and Hartshorne, D. J. (1989) *Biochem. Biophys. Res. Commun.* **159,** 871–877
41. Altroff, H., Schlinkert, R., van der Walle, C., Bernini, A., Campbell, I., Werner, J., and Mardon, H. (2004) *J. Biol. Chem.* **279,** 55995–56003
42. de Vos, A. M., Ultsch, M., and Kossiakoff, A. A. (1992) *Science* **255,** 306–312

---

[3] J. M. de Pereda, unpublished results.